The Benzyl Moiety in a Quinoxaline-Based Scaffold Acts as a DNA Intercalation Switch

Tridib Mahata, Ajay Kanungo, Sudakshina Ganguly, Eswar Kalyan Modugula,
Susobhan Choudhury, Samir Kumar Pal, Gautam Basu,* and Sanjay Dutta*

Abstract: *Quinoxaline antibiotics intercalate dsDNA and exhibit antitumor properties. However, they are difficult to synthesize and their structural complexity impedes a clear mechanistic understanding of DNA binding. Therefore design and synthesis of minimal-intercalators, using only part of the antibiotic scaffold so as to retain the key DNA-binding property, is extremely important. Reported is a unique example of a monomeric quinoxaline derivative of a 6-nitroquinoxa-line-2,3-diamine scaffold which binds dsDNA by two different modes. While benzyl derivatives bound DNA in a sequential fashion, with intercalation as the second event, nonbenzyl derivatives showed only the first binding event. The benzyl intercalation switch provides important insights about molec-ular architecture which control specific DNA binding modes and would be useful in designing functionally important monomeric quinoxaline DNA binders and benchmarking molecular simulations.*

Quinoxaline antibiotics, containing two quinoxaline moi-eties attached to an octadepsipeptide ring (Figure 1 A), are able to bis-intercalate double-stranded DNA (dsDNA) in a sequence-specific manner.[1–3] In addition to studies on synthetic derivatives,[4,5] potent anticancer agents have been designed using the depsipeptide-biquinoxaline scaffold.[6] In contrast, known DNA-binding monoquinoxaline scaffolds are either metal chelates[7] or contain a fused quinoxaline moeity.[8] The DNA binding affinity of the only reported simple synthetic monoquinoxaline DNA-binding scaffold, however, was only moderate.[9] There is a need to develop simpler monoquinoxaline DNA-intercalating small molecules since they can be easily synthesized and derivatized for modulating DNA affinity and targeted delivery. Herein we report the design, synthesis, and DNA binding properties of a series of synthetically accessible small molecules derived
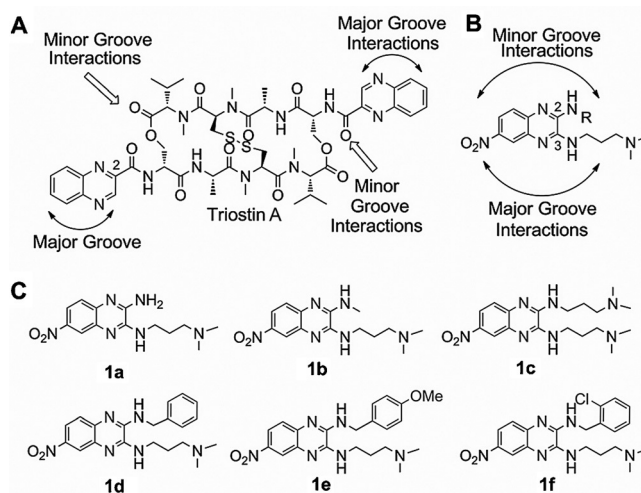

Figure 1. A) Structure of quinoxaline antibiotic triostin A depicting key DNA interactions. B) The nitroquinoxaline-diamine scaffold used in this study with plausible DNA interactions. C) Structures of the six molecules used in this work. Atom numbering of quinoxaline in triostin A is used throughout.

from an unfused monoquinoxaline scaffold, and we identify a unique benzyl switch which controls their DNA-binding modes.

The design of quinoxaline derivatives was inspired by the structure[10] of the dsDNA-bound quinoxaline antibiotic triostin A (Figure 1 A) and the monoquinoxaline derivatives reported by Waring et al.[9] The scaffold contained a triply substituted (C2, C3, and C6) monoquinoxaline (Figure 1 B) with the C6-nitro group as a synthetic handle for C2/C3 substitutions, the C2/C3 quinoxaline amines as potential DNA hydrogen-bond donors, and the C3 propyl dimethyl amine for electrostatic interactions with DNA and to facilitate a snug fit in the minor-groove (alkyl chain). The C2-quinoxaline amine was substituted with various groups ranging from small and simple alkyl groups to bulky aromatic moieties (Figure 1 C). The quinoxaline analogues were syn-thesized using modifications of established methodologies[11] as described in Section S1 in the Supporting Information.

The DNA-intercalation properties of the compounds **1a–f** (Figure 1 C) were probed by an agarose gel shift assay with supercoiled plasmid DNA, a classical test for DNA interca-lation where intercalation-induced unwinding of negatively supercoiled DNA results in a slower moving band.[12] Com-pounds without a benzyl substitution (**1a–c**) showed no discernible band shift (Figure 2 A), whereas those with benzyl substitution (**1d–f**) showed a substantial band shift and

[*] T. Mahata, A. Kanungo, Dr. S. Dutta
Department of Organic and Medicinal Chemistry
CSIR-Indian Institute of Chemical Biology
4 Raja S. C. Mullick Road, Kolkata 700032, WB (India)
E-mail: sanjaydutta@iicb.res.in

S. Ganguly, E. K. Modugula, Dr. G. Basu
Department of Biophysics, Bose Institute
P-1/12 CIT Scheme VIIM, Kolkata 700054 (India)
E-mail: gautam@jcbose.ac.in

S. Choudhury, Dr. S. K. Pal
Department of Chemical, Biological and Macromolecular Sciences
S. N. Bose National Centre for Basic Sciences
Block JD, Sector III SaltLake, Kolkata 700 098 (India)

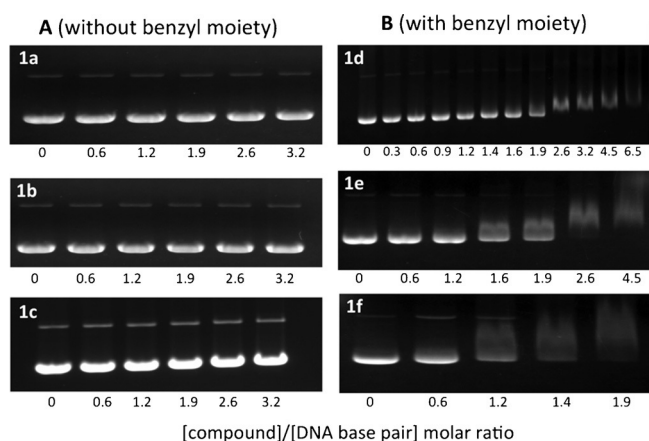Supporting information for this article can be found under:
http://dx.doi.org/10.1002/anie.201511881.

Figure 2. Agarose gel shift assay of supercoiled DNA with the compounds **1a–c** (A) and compounds **1d–f** (B). See Section S2 in Supporting Information for details.

reduced intensity after a certain [ligand]/[DNA] threshold (Figure 2B). The data suggests that benzyl-substituted compounds intercalate supercoiled DNA, a property not shared by nonbenzyl compounds.

Circular dichroism (CD) is an important technique for monitoring small-molecule binding to DNA.[13] As shown in Figure 3, all benzyl-substituted compounds (**1d–f**) displayed induced CD (ICD) in the presence of calf thymus DNA (ct-DNA), whereas compounds without a benzyl group (**1a–c**)
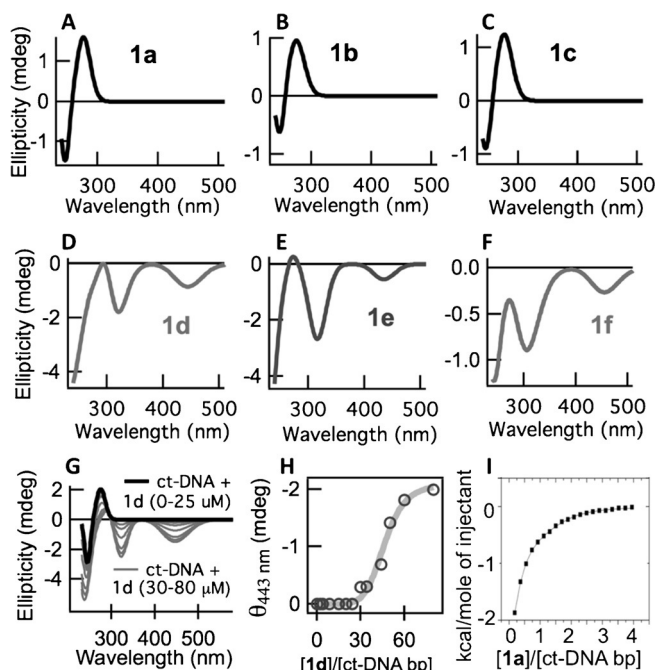

Figure 3. CD spectra of 50 μM **1a** (A), **1b** (B), **1c** (C), **1d** (D), **1e** (E), and **1f** (F) in the presence of 10 μM ct-DNA (bp) in buffer A (10 mM phosphate buffer pH 7.0 with 10 mM NaCl and 1% DMSO) at 25°C. The compounds **1a–f** did not show ICD at this concentration in the absence of DNA. G) Titration of ct-DNA (15 μM) by **1d**. H) $\theta_{443\,nm}$ versus [**1d**]/[DNA] from (G). I) Difference in integrated heat from ITC titrations of **1a** against 50 μM ct-DNA and buffer A as a function of [**1a**]/[ct-DNA].

displayed no ICD. Titration of ct-DNA with **1d** (Figure 3G) generated a sigmoidal growth of ICD (Figure 3H; for the $\lambda = $ 443 nm band) appearing only after [**1d**]/[ct-DNA] ≈ 2. This data suggests a sequential binding model [m(**1d**) + A⇔B; B + n(**1d**) ⇔C] where **1d** first binds ct-DNA (species A) to yield species B (ICD-silent), which then yields species C (with ICD) with more **1d**. A fit of ICD data (solid line in Figure 3H) to the sequential model yielded $<K_{BA}> \approx 414$ μM, $<K_{CB}> \approx 36$ μM, m ≈ 0.4, and n ≈ 4 where $<K_{BA}>$ and $<K_{CB}>$ are average microscopic dissociation constants (see Section S3 in Supporting Information for details).

The ICD-silent first binding event was probed by isothermal calorimetry (ITC) for **1a** (Figure 3I; see Figure S1 for details; other compounds did not yield reliable data because of poor solubility in water). The best fit to ITC data (solid line in Figure 3I) showed an enthalpy-driven binding mode ($K_{d1} \approx 1.6$ μM) involving about 5 bp/ligand, which is consistent with specific DNA binding, and an entropy-driven binding mode ($K_{d2} \approx 10.6$ μM) involving about 0.5 bp/ligand (see Figure S1).

Competitive binding assays, where a small molecule quenches the fluorescence of a DNA-bound fluorophore by displacing it, were performed with **1a–f** against four known DNA binders which show enhanced fluorescence only when DNA-bound: a) DAPI,[14] b) EtBr,[15] c) Qcy-DT,[16] and d) TC.[17] The absorption spectra of **1a–f** (all nonfluorescent in either the presence or in absence of ct-DNA) and the emission spectra of the four fluorophores are shown in Figures S2 and S3, respectively. Overlap of the absorption spectra of **1a–f** and the emission spectra of DNA-bound fluorophores showed that **1a–f** is capable of quenching DAPI fluorescence by FRET (see Section S4).

All compounds quenched DNA-bound DAPI fluorescence in the ICD-silent regime (Figure 4A) up to a [ligand]/[DNA] ≈ 2, thus reflecting the first binding event. Quenching of DAPI fluorescence could either occur by displacement of
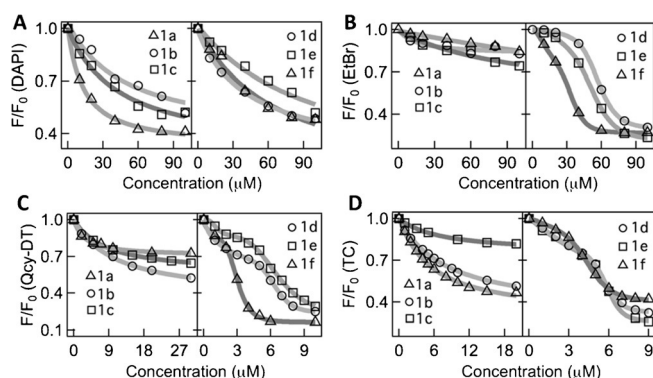

Figure 4. Fluorescence quenching of 10 μM ct-DNA and 10 μM DAPI ($\lambda_{ex} = 338$ nm; A), 20 μM ct-DNA and 10 μM EtBr ($\lambda_{ex} = 480$ nm; B), 10 μM ct-DNA and 2 μM Qcy-DT ($\lambda_{ex} = 564$ nm; C), and 10 μM ct-DNA and 10 μM TC ($\lambda_{ex} = 521$ nm; D) by compounds **1a–f** (in buffer A at 25°C). The solid lines are the best fits to the data using a Langmuir isotherm (A, and the left panels of B, C, and D) or a sequential model (the right panels of B, C, and D). Maximum error along the abscissa is 0.1 units (all fluorescence spectra were corrected for inner filter effect).

DAPI from the minor groove (DAPI is a known minor groove binder),[14] or through FRET by binding to some other sites on DNA (this binding mode cannot be intercalation since no gel shift was observed in Figure 2 A in this regime), or both. Thus, the first binding event, captured by DAPI fluorescence quenching (and by ITC) and common to all compounds, is a non-intercalation event while the second binding event, captured by ICD and exclusive to benzyl compounds, is an intercalation event (significant gel shift in Figure 2B in this regime).

If the benzyl- and the nonbenzyl compounds fundamentally differ in their ability to intercalate DNA then it would be reflected in the displacement assay of DNA-bound EtBr (a known intercalator).[15] Indeed, the two groups show dramatically different EtBr fluorescence quenching patterns. Similar to the ICD data, EtBr fluorescence was quenched (right panel Figure 4B) in a sigmoidal fashion by **1d–f**, thus fitting well with the sequential model, whereas **1a–c** showed little fluorescence quenching (left panel Figure 4B), with the fluorescence decreasing in a hyperbolic fashion. The data suggest that **1d–f** intercalate DNA (displacing EtBr) but not **1a–c**.

Fluorescence quenching profiles of ct-DNA-bound Qcy-DT (Figure 4C) and TC (Figure 4D) were also very different for benzyl and nonbenzyl compounds. The benzyl compounds efficiently quenched Qcy-DT fluorescence in a sigmoidal fashion (90% quenching at 10 μM) but the nonbenzyl compounds showed a canonical hyperbolic quenching with only 30% quenching at 10 μM.

The recurring sigmoidal DNA interaction, observed in gel shift, ICD, and a fluorescence displacement assay, hints at some underlying cooperative phenomenon where intercalation at one DNA site makes intercalation at another site easier, possibly through DNA structural changes. One possibility is that **1a–f** aggregate in aqueous medium and some specific interaction between the aggregate and ct-DNA triggers DNA structural change. Dynamic light scattering (DLS) studies on **1b** and **1d**, in the presence and in absence of DNA (see Figure S4) showed that both formed multimeric aggregates in aqueous buffer. Absorption spectra of **1a–f** (see Figure S2) also showed aggregation. We also investigated plausible DNA intercalating modes by docking **1d** on short DNA sequences (see Figure S5) and they showed **1d** to be an efficient threading intercalator with the quinoxaline ring sandwiched between DNA base pairs and the benzyl ring bulging out towards the minor groove (Figure 5D). The docked structure and the DLS data, together, suggest a model where **1d** first binds DNA and prepares it for intercalation. This binding event (ICD-silent) is not intercalation and probably not groove binding either since minor-groove binding is usually expected to yield a large positive ICD.[18] More **1d** initiates intercalation (Figure 5A→B). Once intercalated, the benzyl group, bulging at side of the minor groove, associates with nearby aggregates of **1d**, thus bringing the DNA and the aggregates into close proximity (Figure 5B→C). This event triggers more intercalation by **1d** (present on the surface of the aggregate) by inducing cooperative conformational changes in the DNA since multiple DNA intercalating sites, originally distant on DNA, are brought
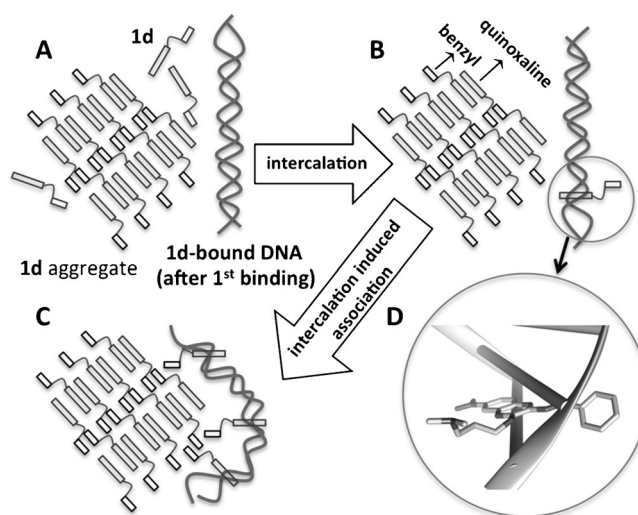

Figure 5. A schematic depiction of a model describing the second binding event where intercalation of **1d** (A→B) to **1d**-bound DNA (after first binding event) triggers cooperative association between DNA and **1d** aggergates (B→C). D) Plausible intercalation modes were obtained from docking studies (see Figure S5).

closer to the **1d** aggregate. According to the model the observed negative ICD arises both from intercalation (weak)[18] and chiral organization of **1d** on the surface of the aggregate resulting from DNA binding. In other words, the aggregate acts a multiple intercalator. Interestingly, **1b** forms aggregates similar to **1d** but cannot intercalate DNA. Thus the presence of the benzyl group is essential for DNA intercalation.

To probe if the quinoxaline derivatives bind shorter ds-DNAs as well, and CD spectroscopy and fluorescence quenching of DNA-bound TC were performed with **1f** (with benzyl substitution) and **1a** (without benzyl substitution) with four self-complementary DNA sequences: A1: $(AT)_6$, C1: $(CG)_6$, D1: $(CG)_2AATT(CG)_2$, and V1: $(CG)_2$-$(AT)_2(CG)_2$. Consistent with the differential ct-DNA binding modes of benzyl- and nonbenzyl-substituted quinoxaline derivatives, **1f** generated an ICD with all four short ds-DNA sequences (Figure 6), whereas **1a** did not (see Figure S6). The corresponding fluorescence quenching of V1 and D1 bound TC (see Figure S7) also showed a clear difference between fluorescence quenching by benzyl (**1f**) and non-benzyl (**1a**) compounds.

The ICD signals for the four short DNA sequences were similar (positive peak at $\lambda \approx 320$ and 400 nm) but not identical (negative peak $\lambda \sim 470$ nm for all but A1), and differed from that of ct-DNA (negative peaks $\lambda \sim 320$ and 443 nm). In addition, the B-DNA-specific positive peak at $\lambda = 270$ nm was substantially reduced in the case of C1 (Figure 6B), thus suggesting a B to Z conformational transition, brought about by **1f**, for $(CG)_6$, but not for others. Interestingly, the negative ICD peak at longer-wavelength for ct-DNA (with benzyl compounds) shows exciton coupling (negative and positive peaks) for shorter DNA (Figure 6), thus suggesting that the ligand binds as a multimer.[18] Multimeric ligand binding is in tune with the model of Figure 5. In summary, CD spectra of
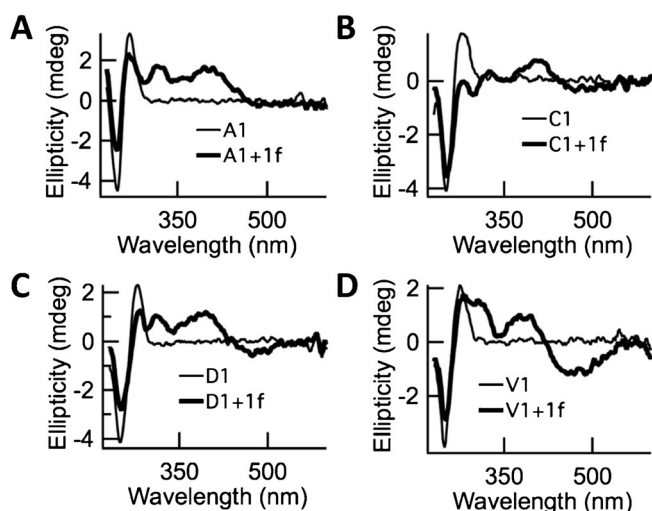
Figure 6. CD spectra of 20 μM dsDNA A1 (A), C1 (B), D1 (C), and V1 (D) in the absence (thin line) and presence (thick line) of 200 μM **1 f** in buffer A at 25 °C.

1 a and **1 f** each with the four short DNA sequences and their comparison with CD spectra obtained with longer ct-DNA showed that the nonbenzyl quinoxalines are incapable of exhibiting ICD. Benzyl-substituted quinoxalines, in contrast, are capable of generating ICD with DNA (both long and short), thus resulting in structures that were sequence and length dependent.

In summary, we have successfully designed simple DNA intercalators based on a quinoxaline scaffold where a unique benzyl switch triggers intercalation following a non-intercalative DNA binding event. The intercalation event is highly cooperative and is ascribed to a DNA structural change resulting from intercalation-induced interaction between the DNA and hydrophobic aggregates of the ligand. Docking showed that the benzyl moiety in the intercalator locks the intercalated state by protruding towards the minor groove, and this could be a reason why nonbenzyl substituents did not show DNA intercalation. The sequential binding is reminiscent of proflavine turning into an intercalated DNA species following groove binding along a kinetic pathway, as revealed from metadynamics studies.[19] The benzyl-substituted quinoxaline scaffold described here is an excellent starting point for design and synthesis of functionally important quinoxaline derivatives. Preliminary data (unpublished) showed that the benzyl-substituted compounds can lead to DNA condensation, DNA double-strand breaks, and cellular DNA damage. Our results could also be useful for benchmarking molecular simulation protocols in an attempt to understand drug–DNA interactions through molecular simulations,[20] especially the differential DNA binding modes of benzyl- and nonbenzyl-substituted compounds.

[1] J. S. Lee, M. J. Waring, *Biochem. J.* **1978**, *173*, 115–128.
[2] M. M. Van Dyke, P. B. Dervan, *Science* **1984**, *225*, 1122–1127.
[3] G. Ughetto, A. H. J. Wang, G. J. Quigley, G. A. van der Marel, J. H. van Boom, A. Rich, *Nucleic Acids Res.* **1985**, *13*, 2305–2323.
[4] J. Tulla-Puche, S. Auriemma, C. Falciani, F. Albericio, *J. Med. Chem.* **2013**, *56*, 5587–5600.
[5] A. J. Hampshire, D. A. Rusling, S. Bryan, D. Paumier, S. J. Dawson, J. P. Malkinson, M. Searcey, K. R. Fox, *Biochemistry* **2008**, *47*, 7900–7906.
[6] D. L. Boger, S. Ichikawa, W. C. Tse, M. P. Hedrick, Q. Jin, *J. Am. Chem. Soc.* **2001**, *123*, 561–568.
[7] K. J. Akerman, A. M. Fagenson, V. Cyril, M. Taylor, M. T. Muller, M. P. Akerman, O. Q. Munro, *J. Am. Chem. Soc.* **2014**, *136*, 5670–5682.
[8] L. M. Wilhelmsson, N. Kingi, J. Bergman, *J. Med. Chem.* **2008**, *51*, 7744–7750.
[9] M. J. Waring, T. Ben-Hadda, A. T. Kotchevar, A. Ramdani, R. Touzani, S. Elkadiri, A. Hakkou, M. Bouakka, T. Ellis, *Molecules* **2002**, *7*, 641–656.
[10] A. H.-J. Wang, G. Ughetto, G. J. Quigley, T. Hakoshima, G. A. Van der Marel, J. H. Van Boom, A. Rich, *Science* **1984**, *225*, 1115–1121.
[11] A. Kanungo, D. Patra, S. Mukherjee, T. Mahata, P. R. Maulik, S. Dutta, *RSC Adv.* **2015**, *5*, 70958–70967.
[12] R. Xu, S. Birke, S. E. Carberry, N. E. Geacintov, C. E. Swenberg, R. G. Harvey, *Nucleic Acids Res.* **1992**, *20*, 6167–6176.
[13] N. C. Garbett, P. A. Ragazzon, J. B. Chaires, *Nat. Protoc.* **2007**, *2*, 3166–3172.
[14] J. J. Kapuscinski, *J. Histochem. Cytochem.* **1990**, *38*, 1323–1329.
[15] J. B. LePecq, C. Paoletti, *J. Mol. Biol.* **1967**, *27*, 87–106.
[16] N. Narayanaswamy, S. Das, P. K. Samanta, K. Banu, G. P. Sharma, N. Mondal, S. K. Dhar, S. K. Pati, T. Govindaraju, *Nucleic Acids Res.* **2015**, *43*, 8651–8663.
[17] N. Narayanaswamy, M. Kumar, S. Das, R. Sharma, P. K. Samanta, S. K. Pati, S. K. Dhar, T. K. Kundu, T. Govindaraju, *Sci. Rep.* **2014**, *4*, 1–10.
[18] M. Eriksson, B. Nordén, *Methods Enzymol.* **2001**, *340*, 68–98.
[19] W. D. Sasikala, A. Mukherjee, *Phys. Chem. Chem. Phys.* **2013**, *15*, 6446–6455.
[20] A. V. Vargiu, A. Magistrato, *ChemMedChem* **2014**, *9*, 1966–1981.